

Influence of short-range and long-range order on the evolution of the morphotropic phase boundary in $\text{Pb}(\text{Zr}_{1-x}\text{Ti}_x)\text{O}_3$

A. M. Glazer

Physics Department, University of Oxford, Parks Road, Oxford OX1 3PU, United Kingdom

P. A. Thomas

Physics Department, University of Warwick, Coventry CV4 7AL, United Kingdom

K. Z. Baba-Kishi, G. K. H. Pang, and C. W. Tai

Department of Applied Physics, The Hong Kong Polytechnic University, Hung Hom, Kowloon, Hong Kong

(Received 27 April 2004; revised manuscript received 6 August 2004; published 23 November 2004)

The local structures of rhombohedral, monoclinic, and tetragonal phases across the morphotropic phase boundary (MPB) of $\text{Pb}(\text{Zr}_{1-x}\text{Ti}_x)\text{O}_3$ are discussed in terms of the progression from short-range to long-range and back to short-range structural order. It is shown that, provided one considers the structures on a suitably small length scale, all three phases can be considered to be monoclinic at the local level and that there need not be any discrete phase boundaries across the MPB. Electron diffraction experiments showing significant variations in diffuse streaking, illustrating the progression from short-range to long-range order, are presented in support of this model. It is suggested that it is the change in the range of structural order that plays the most important role in the increase in electrical and electromechanical properties around the MPB.

DOI: 10.1103/PhysRevB.70.184123

PACS number(s): 77.84.Dy, 77.80.Bh, 63.70.+h, 61.10.-i

I. INTRODUCTION

Recently, considerable interest has been generated in the so-called morphotropic phase boundary (MPB) found in certain perovskite solid solution systems, especially since the discovery of monoclinic phases in the MPB region.¹ Our intention in this paper is to develop a structural model for these materials that provides an explanation for the variation of the structures with composition in terms of changes in the range of local order. We begin with a brief review of the history of the MPB (a fuller review of the recent work has been given by Noheda²).

Lead titanate (PbTiO_3) and lead zirconate (PbZrO_3) form solid solutions $\text{Pb}(\text{Zr}_{1-x}\text{Ti}_x)\text{O}_3$ (PZT) over the whole composition range. The phase diagram (Fig. 1) was established by a number of workers.³⁻⁷ The phase diagram shows that for $x \leq 0.48$ there is an almost vertical boundary between a tetragonal ferroelectric phase F_T with space group $P4mm$ and a rhombohedral ferroelectric phase $F_{R(HT)}$ of space group $R3m$. This boundary is nearly temperature independent and has been termed the ‘‘morphotropic phase boundary’’ or MPB. The work of Shirane *et al.*⁵ established that the MPB lay between $x=0.45$ and 0.4 , while that of Jaffe *et al.*⁸ reported that it was at $x=0.48$.

This idea of a sharp boundary between rhombohedral (R) and tetragonal (T) phases immediately raised the question of how it is possible to pass smoothly from one side to the other when the symmetry of neither phase is subgroup related to the other. Moreover, the large size difference between Zr^{4+} and Ti^{4+} (of approximately 19% in the ionic radius) makes the idea of a MPB defined as a line between two phases seem unlikely. In such situations, one would normally expect to find a two-phase region separating the two solid solutions within the phase diagram. This argument is equivalent to that

used for phase transitions in materials such as BaTiO_3 , where, for example, increasing temperature converts a rhombohedral phase into an orthorhombic phase: The change has to be first order and accompanied by large phase coexistence and thermal hysteresis. The same happens in BaTiO_3 between the orthorhombic and tetragonal phases.

Jaffe, Roth, and Marzullo⁹ discovered interesting properties near the MPB and, in particular, that the piezoelectric coupling factors sharply increased as the MPB was approached. A more detailed investigation¹⁰ found that all the piezoelectric, elastic and dielectric constants rise to a maximum around $x \approx 0.48$. In the years that followed, the dependence of these quantities on composition, temperature, bias-

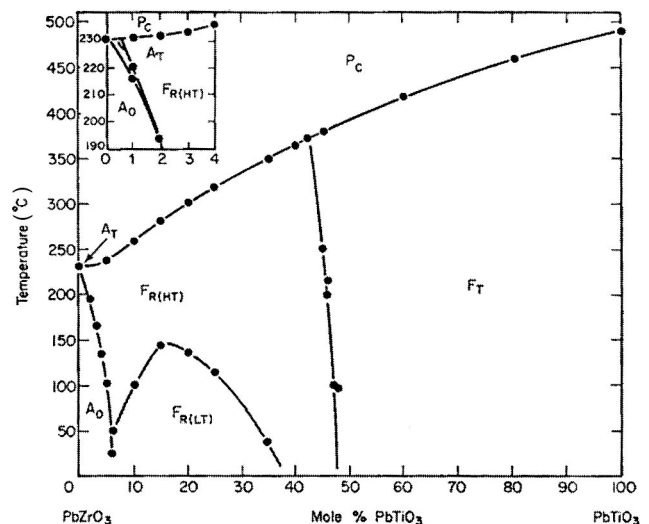


FIG. 1. The phase diagram of $\text{PbZr}_{1-x}\text{Ti}_x\text{O}_3$ after Jaffe, Cooke, and Jaffe (Ref. 8).

ing field, etc., was thoroughly investigated.^{11–14}

Heywang¹⁵ attempted to explain the occurrence of the maximum in the piezoelectric constants by the assumption that a higher degree of domain reorientation is achieved during poling. Isupov¹⁶ tried to explain the phenomenon by assuming the occurrence of an orientational polarization favored by the applied field. The validity of these assumptions was, however, questioned by Dantsiger and Fesenko.¹⁷ Isupov was able to explain the variation of electrical properties with composition by postulating the existence of small islands of differing composition. In particular, the theory gave an increase in polarization close to the MPB, although the magnitude of the increase did not completely fit the experimental measurements. Using a variation of the Devonshire phenomenological theory, he further showed that it was possible for the *T* and *R* phases to coexist over a range of compositions. He also explained the rise of the dielectric constant around the MPB, where the MPB was not a line but a band of certain width depending on various parameters. However, Carl and Härdtl¹⁸ doubted the validity of Isupov's theory because he utilized the results of a calculation by Shirobokov and Khodolenko¹⁹ that were not consistent with the results of the Devonshire theory. Instead, they explained the maximum in the electromechanical activity at the MPB, but did not predict any coexistence of phases. Benguigui²⁰ applied the Devonshire theory to explain both the maximum in the dielectric constant and that orthorhombic (*O*), *T*, and *R* phases may occur near the MPB.

Wersing²¹ assumed a fluctuation of concentration near the MPB, and gave an estimate for the width of a coexistence region of about 8 mol % Ti from an analysis of dielectric measurements of ceramics. Pinczuk²² suggested that the *R* to *T* transition was connected with the softening of an *E*(*TO*) mode, with the mode condensing out at $x \leq 0.47$. This idea was put to the test by Bäuerle, Yacoby, and Richter,²³ who found that while this mode does soften, it does not condense out at the MPB.

Ari-Gur and Benguigui,²⁴ using x-ray diffraction, found that the MPB extended over the composition range $0.49 \leq x \leq 0.64$. The lattice parameters of each phase were constant over the coexistence region. They were unable to measure the rhombohedral angle, as this was too close to 90° to be resolved from the low-angle lines that they were using.

Isupov²⁵ reported an analysis of the characteristic coexistence of *T* and *R* phases, in which he showed that the MPB need not be strictly parallel nor smooth. However, this theory did not explain the experimental results quantitatively. Kakegawa *et al.*²⁶ found that coexistence of phases was absent when PZT was prepared by chemical precipitation techniques, but was present in normal sintered ceramics. They interpreted this effect as being evidence of compositional fluctuations in the ceramics. Mabud²⁷ carried out sintering syntheses of PZT under different firing conditions and was able to minimize the coexistence region to less than 1 mol % Ti by increasing the grain size. Cao and Cross²⁸ proposed a model in which the width of coexistence regions around the MPB is inversely proportional to particle size, suggesting that if a single crystal were available, the boundary would be sharp. Singh *et al.*²⁹ were able to get the width down to about 0.1 mol % Ti using semiwet methods of preparation.

An indication of a way to explain the sequence of phases across the MPB was given by Corker *et al.*³⁰ in 1998, who carried out neutron powder structure analysis of the *R* phase. In this work a model for disordered Pb positions was proposed, which essentially could be interpreted in terms of local monoclinic distortions within individual unit cells. However, the real breakthrough came about with the publications by Noheda *et al.*,^{31–33} in which it was shown that within a narrow region, $0.45 < x < 0.52$, around the MPB there was a monoclinic phase, denoted by M_A (after Vanderbilt and Cohen³⁴ who predicted the existence of the monoclinic phases through an eighth-order Devonshire expansion), of space group symmetry *Cm*, which was consistent with the local symmetry discussed by Corker *et al.* The existence of the M_A phase, which was sandwiched between the *T* and *R* phases, provided a satisfactory explanation of how it was possible to go smoothly from the *R* to the *T* phase. Since space group *Cm* is a subgroup of both *R3m* and *P4mm*, it is possible to pass without disruption from one to the other, *via* the monoclinic group, simply by lowering their symmetries. The intermediate M_A phase has also subsequently been shown to permit an explanation of the increase in piezoelectricity in this region of composition³⁵ through a polarization rotation mechanism. In this model, the key point is that the induced piezoelectric polarization, as represented principally by the direction of displacement of the Pb atoms, is free to rotate within the mirror plane of the *Cm* unit cell, instead of being confined along a particular symmetry axis as in *R3m* and *P4mm*.

Since the important discovery of the monoclinic intermediate, many papers have appeared on this subject. Ragini *et al.*³⁶ also found a monoclinic phase but suggested, in addition, that the *R* phase between $0.47 \leq x \leq 0.38$ was actually monoclinic. They also found evidence for the coexistence of tetragonal and monoclinic phases for $x=0.48$. They gave evidence³⁷ from the presence of superlattice peaks that there exists a second monoclinic phase, which has a unit cell doubled with respect to the *Cm* phase at low temperature in tetragonal PZT. Noheda, Wu, and Zhu,³⁸ using transmission electron microscopy, showed that there was a minority phase in which oxygen octahedra were tilted, thus explaining the superlattice peaks.

It should be noted that similar bridging phases have been found at the MPB between rhombohedral and tetragonal regions in two other important lead-based piezoelectric solid solutions, $\text{PbMg}_{1/3}\text{Nb}_{2/3}\text{O}_3\text{-PbTiO}_3$ (PMN-PT) and $\text{PbZn}_{1/3}\text{Nb}_{2/3}\text{O}_3\text{-PbTiO}_3$ (PZN-PT). In PMN-PT, a monoclinic phase with space group *Pm*, denoted by M_C , has been proposed³⁹ and in PZN-PT, an orthorhombic phase has been suggested.⁴⁰ In all of PZT, PMN-PT, and PZN-PT, a clear boundary between the bridging monoclinic/orthorhombic phase and the *T* phase has been seen. However, no clear boundary between the bridging phase and the *R* phases has been reported.

From the above, it is evident that the MPB has been the focus of considerable attention, especially since the discovery of the monoclinic bridging phase. However, it is true to say that in all of the discussions so far published, virtually no attention has been paid to the disorder, or rather the occurrence of any short-range order, in these materials. Further-

more, it must be realized that in an inherently disordered system such as PZT, the spatial scale with which one describes the structures of the phases is an important parameter that should be taken into account. It is this aspect that we wish to explore here in some detail. We shall show, by the use of stereographic projections to illustrate atomic displacements and structural distortions, that it is possible to account for the sequence of phases $R3m$, Cm , and $P4mm$, so that in fact no distinct phase boundary need be crossed, provided that we use a local structural description. This leads to the conclusion that from a local structural point of view, *there is no morphotropic phase boundary because both the rhombohedral and tetragonal phases (with the exception of pure PbTiO_3) are really monoclinic, but exhibit different degrees of structural disorder*. It is worth noting that our proposal bears a relationship to the models described by Jin *et al.*⁴¹ and Viehland⁴² who, by treating the problem in terms of martensite theory, suggested a way to form an adaptive ferroelectric phase consisting of a coherent mixture of microdomains that average out to be monoclinic. This model was applied to PMN-PT and to PZN-PT. In further support of our model, we also report here transmission electron diffraction studies of a range of PZT compositions spanning the rhombohedral, tetragonal, and the MPB phases. Fuller details of the TEM experiments will be given in a future publication.

II. DESCRIPTION OF AVERAGE STRUCTURES

The basic structure type, namely, perovskite ABO_3 , consists of oxygen octahedra corner-linked along all three pseudocubic directions. Between the octahedra lie the A cations, Pb in this case, and inside the octahedra lie the B cations (either Zr or Ti). This structure is capable of a great many variations, in which cations can be moved off-center and octahedra can be tilted in different ways (Mitchell⁴³ gives a good review). In the following discussion we shall confine ourselves primarily to the PZT phase diagram for $x > 0.1$. We shall refer all structural descriptions to the pseudocubic perovskite unit cell of side $\sim 4 \text{ \AA}$ throughout, except where explicitly stated otherwise.

A. Rhombohedral $R3c$ and $R3m$ phases

The crystal structure of $\text{PbZr}_{0.9}\text{Ti}_{0.1}\text{O}_3$ was studied by Michel *et al.*⁴⁴ with modest precision. In the $F_{R(LT)}$ phase with space group $R3c$, the Pb and Zr/Ti atoms are displaced parallel to each other along $[111]$ to give a polar ferroelectric phase. At the same time, the oxygen octahedra are tilted about $[111]$ with tilt system $a^-a^-a^-$, in the notation of Glazer,⁴⁵ giving rise to a doubling of the unit-cell axes. The $F_{R(HT)}$ phase of space group symmetry $R3m$ is very similar, except that the tilts are lost. For the purposes of our discussion, the $R3m$ phase is simply the same as the $R3c$ phase, but with the octahedral tilts set to zero.

The structure of ceramic $\text{PbZr}_{0.9}\text{Ti}_{0.1}\text{O}_3$ was also studied by Glazer, Mabud, and Clarke⁴⁶ using the Rietveld technique applied to neutron diffraction data. The results of this work were in good agreement with that of Michel *et al.*, but revealed an unusual feature in the anisotropic displacement

parameters ADP (in old terminology, the anisotropic thermal parameters) for the Pb atom. It was consistently found that this was a flattened disk shape oriented with its plane perpendicular to the $[111]$ polar axis. This basic shape was largely independent of temperature, showing that it represented static disorder of the Pb atoms rather than the effect of anisotropic thermal vibrations. Sawaguchi⁶ had earlier suggested a similar ADP for Pb from x-ray powder diffraction measurements.

The Rietveld analysis by Corker *et al.*³⁰ revealed a number of important unusual features of the rhombohedral PZT structures. Using the notation of Megaw and Darlington,⁴⁷ the structural parameters refined were the Pb displacements s , the Zr/Ti displacements t , the tilt angle of the octahedra ω , and the distortion of the octahedral faces d . In addition, from measurements of $90^\circ - \alpha$, where α is the rhombohedral angle, the so-called deformation parameter ξ was calculated; note that this is not obtained from refinement of the atomic positions but directly from the unit cell geometry.

Corker *et al.* found that with increasing Ti concentration x , the parameters ω and d decrease continuously. In the case of ω , the decrease of the tilt angle to zero signifies the transition from the tilted $R3c$ structure to the untilted $R3m$ structure. Since the end-member PbTiO_3 is itself an untilted structure, a tendency for the tilts to disappear with increasing x is expected. The decrease of parameter d is consistent with the structure, as expressed by its internal atomic coordinates, becoming less rhombohedral as a function of x . However, in contrast with the behavior of d , the deformation ξ *increases continuously* over the range of compositions from $x=0.08$ to 0.38 , indicating that the unit cell is becoming increasingly *metrically* rhombohedral. This conflict between the geometrical nature of the unit cell, expressed through ξ , and the internal structural coordinates, expressed through d , is peculiar to PZT: Such behavior has not been seen in any other perovskite. This anomalous behavior suggests an underlying feature of the changes in the average crystal structure of the PZT solid solution that, as yet, is unexplained.

The Corker *et al.* refinements also yielded ADP's for the Pb atom in the shape of a thin disk perpendicular to the $[111]$ Pb displacement direction for all compositions. They explained this by Pb atoms being disordered over three sites slightly off the $[111]$ direction and towards the $\langle 100 \rangle$ directions. This means that *at a local unit cell level* the structure is not actually rhombohedral but is monoclinic with the same space group symmetry as the Cm monoclinic phase proposed by Noheda *et al.* However, the structure is rhombohedral *on average* over all unit cells.

B. Tetragonal $P4mm$ phase

The end member of the PZT series, PbTiO_3 , has a well-determined and simple perovskite type structure.^{48,49} In this structure, the Pb and Ti atoms are displaced parallel to one another along $[001]$ with respect to the center of the oxygen octahedron. The doped tetragonal phase, however, has hardly been studied until recently. X-ray synchrotron measurements⁵⁰ have shown that for the tetragonal phase with $x=0.52$ the ADP's for Pb are disk shaped, but this time

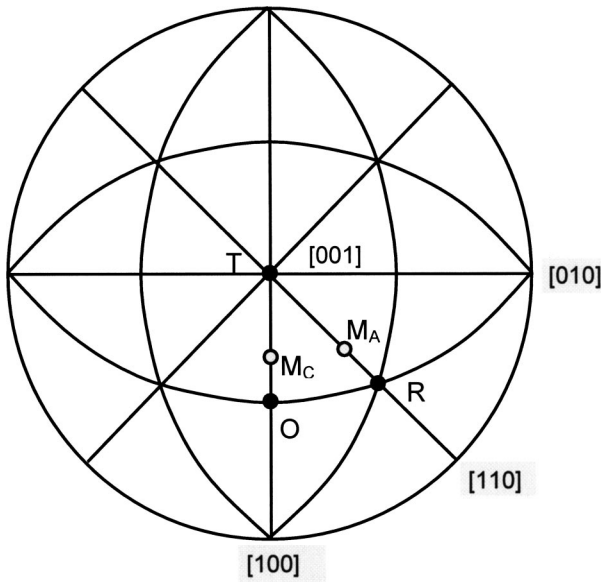


FIG. 2. Stereographic projection of pseudocubic perovskite. The special points marked O , R , and T represent the directions of average Pb displacements for orthorhombic, rhombohedral, and tetragonal phases. A Pb displacement in the direction M_A corresponds to the monoclinic C_m structure.

flattened perpendicular to $[001]$. It was suggested, by analogy with the rhombohedral phase, that this could be explained by occupation by Pb of four sites, displaced slightly along $\langle 110 \rangle$ directions, to give an overall disorder about $[001]$. A similar result for the ADP's has also been seen using neutron diffraction.⁵¹

III. STRUCTURAL CHANGES ACROSS THE MORPHOTROPIC PHASE BOUNDARY

To date, most of the explanations given for the structural changes with composition have been based on considerations of the average crystal structure. The disorder that must be present in all of these structures, apart from in PbTiO_3 , itself, has been largely ignored so far. Below, we describe how the rhombohedral to monoclinic to tetragonal phase changes can be explained by taking this into account.

For this purpose we shall concentrate only on the displacements of the Pb atoms. It is convenient to use stereographic projections to represent the direction of the Pb displacement. Figure 2 shows a cubic (or to be more precise, pseudocubic) stereographic projection with the points O , R , and T marked on it to indicate possible directions for the Pb displacement vectors along $[101]$, $[111]$, and $[001]$, respectively. If we think of the Pb atom as being displaced along the direction denoted R , then the structure would be purely rhombohedral, along O it would be orthorhombic and along T it would be tetragonal.

Figure 3 shows a sequence of models for the Pb displacements. Figure 3(a) denotes the Pb displaced along $[111]$, marked R , with the gray circle indicating the flat disk-shaped ADP. The model in Fig. 3(b) replaces the single Pb by three Pb atoms slightly off the $[111]$ direction and displaced to-

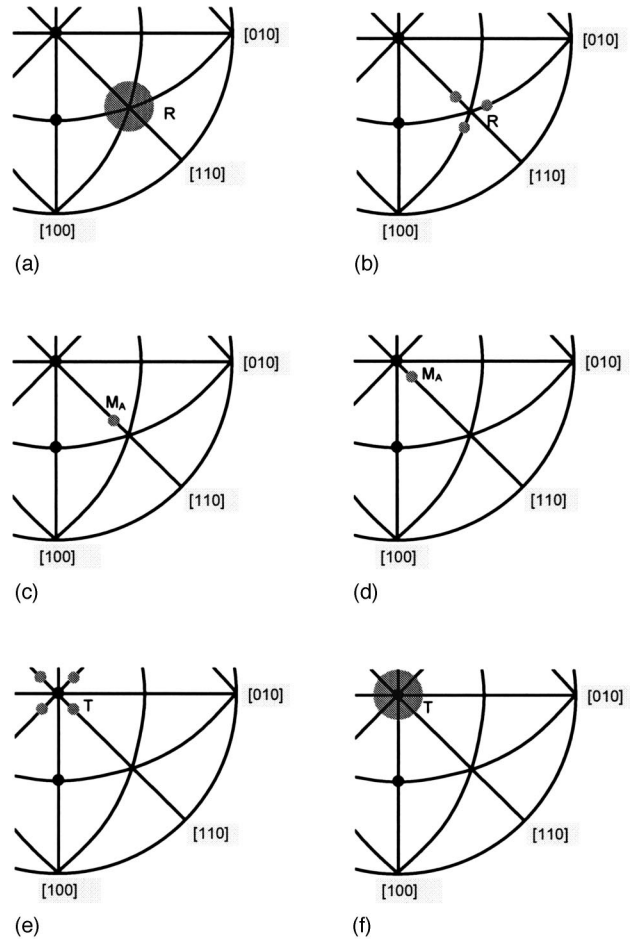


FIG. 3. Part of the stereographic projection showing possible Pb displacements as the Ti concentration increases through the MPB composition. (a) Average R phase with a single Pb displacement along $[111]$ showing a large flat ADP ellipsoid perpendicular to $[111]$. (b) Resolution of Pb displacements in the R phase into three separate components disordered around $[111]$. The space group is still seen in diffraction experiments to be $R3m$. (c) Regions with one component of Pb displacement have now grown to a size exceeding the coherence length of the radiation used in a diffraction experiment. The structure is now seen to be monoclinic M_A . (d) The Pb displacement now is directed closer to the $[001]$ direction. The crystal structure is still seen to be monoclinic M_A . (e) Fourfold disordered arrangement of Pb displacements around $[001]$. The average structure is now seen to be tetragonal $P4mm$. (f) A single average Pb displacement along $[001]$ but with a large flat ADP perpendicular to $[001]$. The structure is now seen to be tetragonal $P4mm$.

wards the $[001]$, $[010]$, $[100]$ directions, with equal $1/3$ occupancies of the three sites. In Fig. 3(c), only one of the three sites is occupied, in which case the structure of the resulting crystal is monoclinic with space group C_m , i.e., the phase usually denoted by M_A . In this model, the Pb displacement is free to move anywhere along the R - T zone, thus providing a mechanism for the high piezoactivity in this region through polarization rotation. Figure 3(d) has the Pb displacement still consistent with monoclinic symmetry but positioned closer to the $[001]$ direction. Figure 3(e) shows the Pb disordered over four sites around $[001]$, each with $1/4$ occupancy,

making the crystal structure now average to tetragonal $P4mm$ symmetry. In Fig. 3(f), the four disordered sites are collapsed to a single Pb site, which is displaced along [001] and has its ADP in the form of a flat disk perpendicular to [001], consistent with the findings of Noheda *et al.*⁵⁰

It should be emphasized that in any scattering or spectroscopic experiment, for example, x-ray or neutron diffraction, Raman scattering or NMR, the details of the structural observations depend upon the spatial scale of the probe compared with the spatial scale of the structural features themselves. In x-ray and neutron diffraction, the coherence length, Λ , of the probing radiation is large ($\sim 0.1-1 \mu\text{m}$), so that structural information obtained from the Bragg peaks is an average over the whole crystal. NMR, however, is a local probe on the scale of the chemical bond and Raman scattering is sensitive to nanoscale structure. Each technique, therefore, provides a different view of the true structure of the material and in disordered structures, the nature of these differences is particularly important.

In general, x-ray, neutron, or electron diffraction may give rise to a pattern consisting of sharp Bragg peaks, indicative of the average crystal structure, superimposed on a weak diffuse background, signifying the presence of short-range order. The presence of diffuse scattering means that there are ordered regions distributed throughout the crystal whose size is less than the coherence length Λ .

In Fig. 3(b) there is disorder of the Pb atoms over three sites, meaning that there are small (perhaps just a few unit cells across) monoclinic regions in which there are correlated Pb displacements in a particular direction away from [111] but toward [001]. In any *one* of these regions the Pb atom is displaced along just *one* of the three possible directions. When these regions are smaller than Λ , they produce a significant diffuse component to the diffraction. Structure determination using the Bragg intensities alone results in a structure with the Pb atom displaced along [111] with an ADP in the form of a flat disk perpendicular to [111] or, equivalently, with a three-site disorder of Pb atoms of 1/3rd weight just off the [111] direction. This picture coincides with the observation of the $R3c$ and $R3m$ phases by Corker *et al.*

Suppose now that for $x < 0.48$ as the Ti concentration x increases, the small ordered regions increase in size until they become larger than Λ . In this case, the diffuse scattering due to the Pb atoms will tend to weaken as the range of order increases. The crystal then consists of a mixture of three types of regions of size greater than Λ , in which Pb displacements are ordered along any one of [100], [010], and [001]. The diffraction pattern thus obtained will be that from a crystal with threefold twinning of the structure. It can be seen from this argument that this sort of twinning is no more than short-range order that has grown to become long-range order, and that it is only the coherence length of the diffracting radiation that determines which one is observed. Structure refinement of this set of diffraction data would conclude that the structure was twinned monoclinic with space group Cm [Fig. 3(c)] i.e., a separate monoclinic phase, that is distinct from the rhombohedral phase.

Suppose now that when $x > 0.48$ the Pb displacements approach closer to the [001] direction [Fig. 3(d)] and, at the

same time, the range of order decreases. The description of the structure remains as monoclinic M_A . However, once the average size of the ordered regions falls below Λ , the diffraction pattern from this crystal will indicate a tetragonal structure with Pb atoms disordered over four sites about [001] [Fig. 3(e)] and the diffuse component to the diffraction pattern will therefore reappear. Note that in the small individual regions of size $< \Lambda$, the structure is still monoclinic, but it averages out to be tetragonal overall. If the structure is now refined with a single Pb atom displaced along [001], the ADP's will form a flat disk perpendicular to [001], as seen by Noheda *et al.*⁵⁰ Finally, as x increases still further, one could imagine that this flat disk shrinks until it forms a point at T in the stereographic projection, whence we obtain the observed tetragonal PbTiO_3 structure.

It can be seen from the above argument that by considering the growth and subsequent reduction of regions of short-range order for the Pb displacements, it is possible to pass smoothly across the phase diagram from the R phase to the T phase. The monoclinic phase M_A is then seen simply as the interval where the monoclinic regions, which are originally at the local unit cell level in the R and T phases, have grown to a size sufficient that diffraction techniques see a distinct phase of monoclinic symmetry.

As well as offering a way of explaining the phase diagram of PZT, there is further experimental evidence in favor of our model. For instance, the work of Ragini *et al.*³⁶ found little evidence for a monoclinic-rhombohedral boundary and indeed they have already questioned the existence of a distinct rhombohedral phase. Furthermore, the observation of an apparent R - T coexistence region in the phase diagram that varies with the method of sample preparation is consistent with the notion of growing regions of short-range order since this would depend critically on the way that the crystallites of PZT are formed. In addition, if one were to use techniques that measure only the local environment of Pb, we would expect to find that it would look monoclinic and that there would be little change across the phase diagram.

In order to understand the driving force for the appearance of short-range order, its subsequent change toward long-range order, and then back to short-range order, we have computed the bond valence between Pb and neighboring oxygens in the crystal structure as a function of composition. The bond valence sum BVS^{57} for a cation coordinated by anions is given by

$$\text{BVS} = \sum_X e^{(R_0 - R_{A-X})/b},$$

where R_{A-X} are the bond lengths between anion and cation. R_0 and b are values that have been obtained empirically from the study of a large number of ionic compounds.⁵⁸

Figure 4 uses the values for the Pb and O positions taken from Corker *et al.*³⁰ and shows that for Ti concentrations between $x=0.1$ and $x=0.4$ the Pb is strongly underbonded, with the underbonding becoming even worse toward the MPB region. This indicates that the structure, as far as the Pb-O bonds are concerned, becomes unstable on approaching the MPB. The final point at $x=0.46$ is taken from Frantti *et al.*,⁵² who pointed out that at the MPB one normally ob-

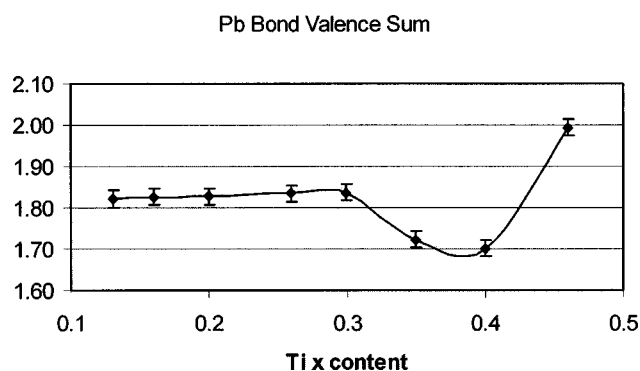


FIG. 4. Bond valence calculations for Pb-O bonds as a function of Ti content, computed from the room-temperature data for the average crystal structure of Corker *et al.* (Ref. 30) (x between 0.13 and 0.40) and from Frantti *et al.* (Ref. 52) ($x=0.46$).

tains a mixture of monoclinic and rhombohedral phases. The interesting result here is that bond valence calculation now gives a value much closer to the ideal value of 2 for Pb, despite all the structural parameters (s , t , d , ω , and ξ) being close to those found in the R phase for the $x \sim 0.3$ composition of Corker *et al.* The principal difference in the Frantti *et al.* structure is that the unit cell volume is approximately 2.5% smaller, thus bringing three apical oxygens into closer contact with Pb, and satisfying the bond valence criterion. The lateral shifts in the R phase are an attempt by Pb to improve its bond valency (for instance for $x=0.35$, the bond valence sum changes from 1.72 to 1.83), although within this phase ideal bond valence is never achieved. In the rhombohedral structure found by Frantti *et al.*, however, there is no evidence of the lateral shifts of Pb, but instead the Pb is displaced only along $[111]$ in order to approach three oxygen atoms, thus creating a more stable bonding situation, with the structure now fully ordered. Thus in the MPB region we find monoclinic and rhombohedral phases, both with long-range ordered structures, in contrast to the short-range order in the rhombohedral R phase with lower Ti content. It is tempting therefore to consider the rhombohedral phase observed in the MPB region as being distinct from that in the R region of the phase diagram.

In the tetragonal region, we again find an improvement in the bond valence for Pb when comparing the average, disordered structure (1.93), with one in which local monoclinic displacements are considered (1.97). In the monoclinic phase we find an improvement in bond valence as temperature is decreased (from 1.90 to 1.98).

IV. PRELIMINARY ELECTRON DIFFRACTION EXPERIMENTS

In order to investigate the nature of diffuse scattering in $\text{Pb}(\text{Zr}_{1-x}\text{Ti}_x)\text{O}_3$ across the phase diagram, ceramic samples were synthesized, corresponding to the phase diagram published by Jaffe *et al.*⁸ These were prepared by a mixed-oxide route. The precursors, PbO (Acros, 99.9%), ZrO_2 (Acros, 98.5%), and TiO_2 (BDH, 98%), were weighed in stoichiometric ratios and mixed by ball milling in ethanol with zir-

conia media for four hours. The mixed powder was calcined at 850°C for two hours and then milled for a further two hours. A binder, 5 wt. % polyvinyl alcohol (PVA), was added to the powder. After cold pressing the resultant pellet was submerged in calcined powder of the same composition in an alumina crucible and sintered at 1200°C for two hours. The compositions synthesized were $x=0.30, 0.46, 0.47, 0.48,$ and 0.70 (denoted 70/30, 54/46, 53/47, 52/48, and 30/70, respectively). Electron diffraction was carried out using a JEOL 2010 transmission electron microscope, operating at 200 kV. The specimens were mechanically ground and polished to a thickness of about $40\ \mu\text{m}$, dimpled and subsequently ion milled. Careful examination showed that single-phase PZT was obtained at each composition, with no evidence of other phases, such as pyrochlore. This agrees with Frantti *et al.*,⁵² who pointed out that it appears that solid-state preparation of PZT can produce single-phase material whereas, surprisingly, sol-gel methods do not.

Figure 5 shows a series of transmission electron diffraction patterns from the various ceramic samples of $\text{Pb}(\text{Zr}_x\text{Ti}_{1-x})\text{O}_3$ across the phase diagram. In indexing the diffraction patterns, we have assumed pseudocubic perovskite axes throughout, for convenience of comparison. The Kikuchi map included in this figure is to enable the locations where the diffraction patterns originate to be identified.

Starting with the pattern with the $[731]$ zone axis for the 70/30 compound, marked C in the Kikuchi map, the most notable feature is the presence of significant polarized diffuse streaking that lies almost continuously in two different directions, joining certain Bragg peaks together. The presence of continuous polarized streaks in two directions is indicative of cross sections of diffuse reflections in two different planes. The diffuse streaks originate from short-range order in two dimensions, i.e., small planar regions of order oriented normal to the directions of the streaks.

Inspection of the $[731]$ diffraction patterns for 54/46 and 53/47 compositions, also recorded along zone axis C , close to the MPB, reveals a reduction in the intensity of the streaks. Similarly, the diffraction pattern recorded for the MPB composition 52/48 (monoclinic structure) shows a significant reduction in diffuse scattering, illustrating the loss of the planar polarized short-range order observed in the rhombohedral state.

On passing through the MPB and its vicinity into the tetragonal state, diffuse streaking returns, illustrating a greater level of short-range order compared with the MPB compositions. However, here the diffuse intensity is unpolarized and less localized than in the diffraction pattern from the rhombohedral state. This is indicative of a more generalized short-range order rather than the highly oriented planar ordering seen in the rhombohedral state.

The above studies were repeated on a different zone axis $[210]$ marked B in the Kikuchi map. In the R phase there is polarized diffuse streaking, but its intensity is weaker compared with the diffuse streaking along $[731]$, zone axis C . It is also less localized. For the monoclinic compositions the diffuse scattering is almost absent, assuming that we ignore the circular diffuse scattering originating from fine sputtered particles on the sample. The diffraction pattern recorded

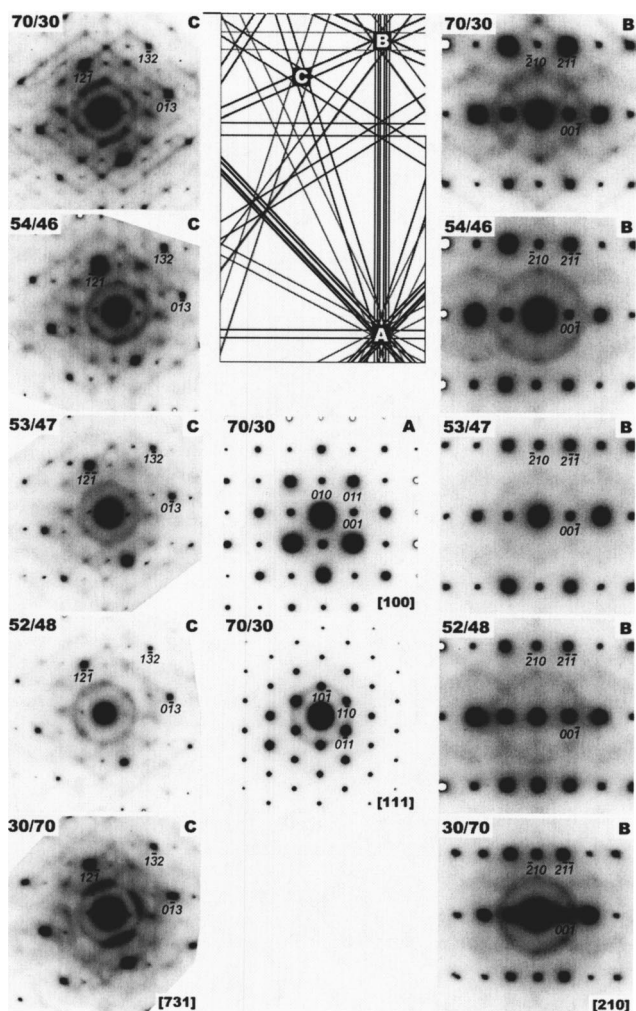


FIG. 5. Electron diffraction patterns recorded along the zone axes *A*, *B*, and *C* shown on the Kikuchi map (top center) corresponding to the rhombohedral (*R*), monoclinic (*M_A*), and tetragonal (*T*) states, respectively of $\text{PbZr}_{1-x}\text{Ti}_x\text{O}_3$. The compositions are shown on the top left corner of each image and the corresponding zone axis is indexed on the bottom right corner of each image. All the images were recorded on photographic films and care was taken to ensure that the background intensities in the negatives remained similar. The intensity differences depicted on the images are therefore reliable. The diffraction images are shown as negatives in order to make the diffuse scattering clearer to the eye.

from the composition 30/70 exhibits some small degree of increased unpolarized diffuse streaking. Compared with the level of diffuse scattering observed along [731], composition 70/30, that along [210] is small for the same composition.

The electron diffraction patterns recorded from one rhombohedral, three MPB (or close to MPB), and one tetragonal composition, along the zone axes marked *C* and *B* in the Kikuchi map, show consistent results. In the rhombohedral composition, diffuse streaking is narrow and sharp and possesses a two-dimensional configuration, illustrating a tendency for planar ordering. In the compositions that fall either on the MPB or in its vicinity, significant reduction in the intensity of the diffuse scattering occurs, consistent with a state of increased long-range order. In the tetragonal state,

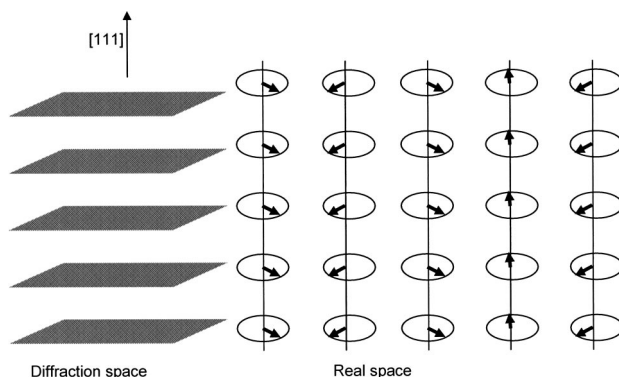


FIG. 6. Schematic diagram illustrating the relationship between the existence of diffuse planes of scattering and correlations between Pb displacements. In diffraction space, thin planes of diffuse scattering perpendicular to $\langle 111 \rangle$ directions are observed passing through the Bragg points. In real space, this suggests Pb displacements that have little or no correlation between adjacent chains: In any one chain, Pb may be displaced in one of three possible directions perpendicular to the chain axis.

some degree of generalized diffuse scattering together with some streaking return, suggesting a reversion to a more short-range ordered state away from the MPB.

An important point to note is that the streaks and other diffuse scattering are always observed to be strongest along high-order zone axes. Diffraction patterns recorded along low-order axes consistently fail to show any diffuse scattering or streaking. Earlier extensive studies of $\text{Pb}(\text{Zr}_{1-x}\text{Ti}_x)\text{O}_3$ carried out by transmission electron microscopy also showed a lack of diffuse scattering along low-order zone axes.⁵³ To show that this is also the case in our experiments, diffraction patterns recorded along the [100] zone axis, marked *A* in the Kikuchi map, and the [111] direction for the 70/30 sample in the *R* phase, are shown in Fig. 5. There is no observable diffuse streaking in these patterns, but only the diffuse ring resulting from fine sputtered surface particles. This loss of diffuse scattering toward the center of reciprocal space indicates that the short-range order originates from ordered cation displacements rather than from regions of chemical substitution, such as that caused, for example, by segregation between Zr- and Ti-containing regions.

Careful examination of the diffuse streaks in the *R* phase shows that they are slices through periodic thin planes of scattering oriented perpendicular to $\langle 111 \rangle$ directions. This implies that in real space along any particular [111] direction, there exist chains of long-range correlations of Pb displacements, but with little correlation between neighboring chains. Figure 6 illustrates this relationship schematically. We should emphasize here, that although we have described the correlations between displacements as if they were static, it is possible that they are dynamic in origin with the displacements fluctuating between each of the three possible sites. Diffraction experiments such as those used here cannot distinguish between static and dynamic fluctuations. Interestingly our model is analogous to that proposed for BaTiO_3 in the classic paper by Comès *et al.*,⁵⁴ except that there the correlated chains were found to be along the $\langle 100 \rangle$ direc-

tions. Our model thus suggests that, on approaching the MPB, the correlations grow and extend between neighboring chains until they have formed three-dimensionally correlated monoclinic regions large enough to scatter separately.

The discussion up until this point has concentrated exclusively on the role of Pb in the short-range order of PZT. It must also be considered that the extent and spatial range of any Zr/Ti ordering that is present also plays a role. For example, do the Zr and Ti ions form clusters that are either Zr-rich or Ti-rich, or are the Zr and Ti ions distributed randomly through all the unit cells in a grain of PZT? This question has been almost entirely ignored in recent literature. NMR studies⁵⁵ however, suggest that the substitution of Ti by Zr in PbTiO₃ is not completely random but is such that Ti-O-Ti chains, on the scale of a couple of unit cells at least, tend to be preserved in the (001) plane. The NMR results also indicate that the essential nature of the Ti environment in its oxygen octahedron is preserved for concentrations of Zr up to and including the MPB, meaning that the mixing of PbZrO₃ unit cells with PbTiO₃ unit cells (in the *T* and *M* phase compositions) does not reduce the ferroelectric displacement of Ti. This is consistent with the refinements of Corker *et al.* for the *R* phase, in which the Ti positions exhibited polar displacements whereas the Zr's did not. The refinements of the *R* phase are not conclusive concerning Ti/Zr ordering but no disorder of either ion was required to fit the neutron diffraction data. From a unit cell size-matching point of view, since Zr is considerably larger than Ti, a truly random distribution of both species in the structure seems improbable. However, in unit cells containing Ti, the evidence is that the Ti atom is displaced along [111] toward one of the oxygen atoms. This causes the unit cell to be slightly distorted and with an increased volume over one in which the displacement were absent. The volume of such a polar Ti-containing unit cell would then be closer to one containing the larger but undisplaced Zr atom, thus facilitating size-matching between chemically different unit cells.

V. SUMMARY

In this paper we have concentrated on the roles of short- and long-range structural order in the lead displacements in explaining the sequence of PZT phases from rhombohedral to tetragonal through the MPB. Our picture, which involves a gradual change in the range of order as a means to develop individual phases, fits observed behavior more closely than one in which there are distinct long-range structures separated by sharp phase boundaries.

For instance, as pointed out by Kisi *et al.*,⁵⁶ the transition from the *R* to *M_A* phases should be discontinuous, whereas the experimental evidence based on structural refinement suggests that there is no sharp boundary between the two phases. Similarly, it is known that the dielectric constant rises from about 200 in the rhombohedral region to 1300 and then drops again through the MPB. This too is consistent with a smooth increase in structural order followed by a subsequent decrease in order with change of composition.

We point out that our model better fits the observed electromechanical behavior of PZT through the MPB. The peaks in piezoelectric constants and coupling factors are observed to span a wide composition range much larger than MPB region. If piezoactivity were associated with polarization rotation in the monoclinic phase alone it should be sharper. We suggest that it is the growth and then disappearance of long-range order with composition that is more important in determining such properties.

ACKNOWLEDGMENTS

A.M.G. and P.A.T. are grateful to the Engineering and Physical Sciences Research Council for a grant during which this work was carried out. The authors thank R. Withers (ANU, Canberra, Australia) for useful advice.

-
- ¹B. Noheda, D. E. Cox, G. Shirane, J. A. Gonzalo, L. E. Cross, and S.-E. Park, *Appl. Phys. Lett.* **74**, 2059 (1999).
- ²B. Noheda, *Curr. Opin. Solid State Mater. Sci.* **6**, 27 (2002).
- ³G. Shirane and A. Takeda, *J. Phys. Soc. Jpn.* **7**, 5 (1952).
- ⁴G. Shirane and K. Suzuki, *J. Phys. Soc. Jpn.* **7**, 333 (1952).
- ⁵G. Shirane, K. Suzuki, and A. Takeda, *J. Phys. Soc. Jpn.* **7**, 12 (1952).
- ⁶E. Sawaguchi, *J. Phys. Soc. Jpn.* **8**, 615 (1953).
- ⁷H. M. J. Barnett, *J. Appl. Phys.* **33**, 1606 (1962).
- ⁸B. Jaffe, W. R. Cook, and H. Jaffe, *Piezoelectric Ceramics* (Academic Press, London, 1971).
- ⁹B. Jaffe, R. S. Roth, and S. J. Marzullo, *J. Appl. Phys.* **25**, 809 (1954); B. Jaffe, R. S. Roth, and S. J. Marzullo, *J. Res. Natl. Bur. Stand.* **55**, 239 (1955).
- ¹⁰D. A. Berlincourt, C. Cmolik, and H. Jaffe, *Proc. IRE* **48**, 220 (1960).
- ¹¹D. A. Berlincourt, D. R. Curran, and H. Jaffe, in *Physical Acoustics*, edited by W. P. Mason, Vol. I-A (Academic Press, New York, 1964).
- ¹²C. E. Land, G. W. Smith, and C. R. Westgate, *IEEE Trans. Sonics Ultrason.* **11**, 8 (1964).
- ¹³H. M. Berlincourt, *J. Acoust. Soc. Am.* **36**, 515 (1964).
- ¹⁴N. Uchida and T. Ikeda, *Jpn. J. Appl. Phys.* **4**, 867 (1965).
- ¹⁵W. Heywang, *Z. Angew. Phys.* **19**, 473 (1965).
- ¹⁶V. A. Isupov, *Sov. Phys. Solid State* **12**, 1084 (1970).
- ¹⁷A. Y. Dantsiger and E. G. Fesenko, *J. Phys. Soc. Jpn.* **28**, 325 (1970).
- ¹⁸K. Carl and K. H. Härdtl, *Phys. Status Solidi A* **8**, 87 (1971).
- ¹⁹M. Y. Shirobokov and L. P. Khodolenko, *Zh. Eksp. Teor. Fiz.* **21**, 1239 (1951).
- ²⁰L. Benguigui, *Solid State Commun.* **11**, 825 (1972).
- ²¹W. Wersing, *Ferroelectrics* **7**, 163 (1974).
- ²²A. Pinczuk, *Solid State Commun.* **12**, 1035 (1973).
- ²³D. Bäuerle, Y. Yacoby, and W. Richter, *Solid State Commun.* **14**, 1137 (1974).
- ²⁴P. Ari-Gur and L. Benguigui, *Solid State Commun.* **15**, 1077

- (1974); P. Ari-Gur and L. Benguigui, *J. Phys. D* **8**, 1856 (1975).
- ²⁵V. A. Isupov, *Sov. Phys. Solid State* **18**, 529 (1976).
- ²⁶K. Kakegawa, J. Mohri, T. Takahashi, H. Yamamura, and S. Shirasaki, *Solid State Commun.* **24**, 769 (1977).
- ²⁷S. A. Mabud, Ph.D. thesis, University of Cambridge (1978).
- ²⁸W. Cao and L. E. Cross, *Phys. Rev. B* **47**, 4825 (1993).
- ²⁹A. P. Singh, S. K. Mishra, D. Pandey, Ch. D. Prasad, and R. J. Lal, *J. Mater. Sci.* **28**, 5050 (1993).
- ³⁰D. L. Corker, A. M. Glazer, R. W. Whatmore, A. Stallard, and F. J. Fauth, *J. Phys.: Condens. Matter* **10**, 6251 (1998).
- ³¹B. Noheda, D. E. Cox, G. Shirane, J. A. Gonzalo, L. E. Cross, and S.-E. Park, *Appl. Phys. Lett.* **74**, 2059 (1999).
- ³²B. Noheda, J. A. Gonzalo, A. C. Caballero, C. Moure, D. E. Cox, and G. Shirane, *Ferroelectrics* **237**, 237 (2000).
- ³³B. Noheda, D. E. Cox, G. Shirane, R. Guo, B. Jones, and L. E. Cross, *Phys. Rev. B* **63**, 014103 (2000).
- ³⁴D. Vanderbilt, and M. H. Cohen, *Phys. Rev. B* **63**, 094108 (2001).
- ³⁵L. Bellaiche, A. Garcia, and D. Vanderbilt, *Phys. Rev. Lett.* **84**, 5427 (2000).
- ³⁶R. R. Ragini, S. K. Mishra, and D. J. Pandey, *J. Appl. Phys.* **92**, 3266 (2002).
- ³⁷R. R. Ragini, S. K. Mishra, D. J. Pandey, H. Lemmens, and G. van Tendeloo, *Phys. Rev. B* **64**, 054101 (2001).
- ³⁸B. Noheda, L. Wu, and Y. Zhu, *Phys. Rev. B* **66**, 060103 (2002).
- ³⁹A. K. Singh and D. J. Pandey, *Phys. Rev. B* **67**, 064102 (2003).
- ⁴⁰D. La-Orautapong, B. Noheda, Z.-G. Ye, P. M. Gehring, J. Toulouse, D. E. Cox, and G. Shirane, *Phys. Rev. B* **65**, 144101 (2002).
- ⁴¹Y. M. Jin, Y. U. Wang, A. G. Khachatryan, J. F. Li, and D. J. Viehland, *J. Appl. Phys.* **94**, 3629 (2003).
- ⁴²D. Viehland, *J. Appl. Phys.* **88**, 4794 (2000).
- ⁴³R. H. Mitchell, *Perovskites, Modern and Ancient* (Almaz Press, Thunder Bay, Ontario, 2002).
- ⁴⁴C. Michel, J.-M. Moreau, G. D. Achenbach, R. Gerson, and W. J. James, *Solid State Commun.* **7**, 701 (1969); **7**, 865 (1969).
- ⁴⁵A. M. Glazer, *Acta Crystallogr., Sect. A: Cryst. Phys., Diffr., Theor. Gen. Crystallogr.* **28**, 3384 (1972); **31**, 756 (1975).
- ⁴⁶A. M. Glazer, S. A. Mabud, and R. Clarke, *Acta Crystallogr., Sect. B: Struct. Crystallogr. Cryst. Chem.* **34**, 1060 (1978).
- ⁴⁷H. D. Megaw and C. N. W. Darlington, *Acta Crystallogr., Sect. A: Cryst. Phys., Diffr., Theor. Gen. Crystallogr.* **31**, 161 (1975).
- ⁴⁸G. Shirane, R. Pepinsky, and B. C. Frazer, *Phys. Rev.* **97**, 1179 (1955); G. Shirane, R. Pepinsky, and B. C. Frazer, *Acta Crystallogr.* **9**, 131 (1956).
- ⁴⁹A. M. Glazer and S. A. Mabud, *Acta Crystallogr., Sect. B: Struct. Crystallogr. Cryst. Chem.* **B34**, 1065 (1978).
- ⁵⁰B. Noheda, J. A. Gonzalo, L. E. Cross, R. Guo, S.-E. Park, D. E. Cox, and G. Shirane, *Phys. Rev. B* **61**, 8687 (2000).
- ⁵¹J. Frantti, J. Lappalainen, S. Eriksson, V. Lantto, S. Nishio, M. Kakihana, S. Ivanov, and H. Rundlöf, *Jpn. J. Appl. Phys., Part 1* **39**, 5697 (2000).
- ⁵²J. Frantti, S. Eriksson, S. Hull, V. Lantto, H. Rundlöf, and M. Kakihana, *J. Phys.: Condens. Matter* **15**, 6031 (2003).
- ⁵³D. Viehland, *Phys. Rev. B* **52**, 778 (1995).
- ⁵⁴R. Comès, M. Lambert, and A. Guinier, *Acta Crystallogr., Sect. A: Cryst. Phys., Diffr., Theor. Gen. Crystallogr.* **A26**, 244 (1970).
- ⁵⁵A. Baldwin, Ph.D. thesis, University of Warwick (2003); A. Baldwin, R. Dupree, and P. A. Thomas, *Proceedings of the 10th European Meeting on Ferroelectricity* (Cambridge Publications, Cambridge, U.K., 2003).
- ⁵⁶E. H. Kisi, R. O. Piltz, J. S. Forrester, and C. J. Howard, *J. Phys.: Condens. Matter* **15**, 3631 (2003).
- ⁵⁷See for example I. D. Brown, *The Chemical Bond in Inorganic Chemistry—The Bond Valence Model*, IUCr Monographs on Crystallography 12 (Oxford University Press, New York, 2002).
- ⁵⁸In our calculation we found it convenient to carry out the calculations using the following web page: kristall.uni_mki.gwdg.de/softbv/index.html